Published in final edited form as:

FASEB J. 2003 November ; 17(14): 1996–2005. doi:10.1096/fj.03-0122com.

Adaptive differences in the structure and macromolecular compositions of the air and water corneas of the "four-eyed" fish (*Anableps anableps)*

SHIVALINGAPPA K. SWAMYNATHAN[*], **MARY A. CRAWFORD**[†], **W. GERALD ROBISON JR.**[‡], **JYOTSHNABALA KANUNGO**[*], and **JORAM PIATIGORSKY**[*,1]

[*]Laboratory of Molecular and Developmental Biology, National Eye Institute, NIH, Bethesda, Maryland, USA

[†]Laboratory of Immunology, National Eye Institute, NIH, Bethesda, Maryland, USA

[‡]Laboratory of Mechanisms of Ocular Diseases, National Eye Institute, NIH, Bethesda, Maryland, USA

Abstract

The water meniscus bisects the eyes of the "four-eyed" fish *Anableps anableps*, resulting in simultaneous vision in air and water. We compare the structure and macromolecular compositions of the *Anableps* dorsal (air) and ventral (water) corneas with the fully aquatic zebrafish cornea. The *Anableps* dorsal corneal epithelium is thicker (>20 cell layers), flatter (~1.94 mm radius of curvature), and contains ~15-fold more glycogen (0.16 μg/μg water-soluble protein) than the ventral corneal epithelium (5–7 cell layers; ~1.63 mm radius of curvature; 0.01 μg glycogen/μg water-soluble protein), which resembles the zebrafish corneal epithelium. Gelsolin is the major water-soluble protein in the zebrafish (~50%) and *Anableps* dorsal (~38%) and ventral (~21%) corneal epithelia, suggesting that gelsolin was recruited for high corneal expression before these two species diverged at least 100 million years ago and that abundant corneal gelsolin is not limited to aquatic vision. *Anableps* gelsolin, deduced from its cDNA, is 57% identical to zebrafish gelsolin. Paucity of *Anableps* corneal F-actin (consistent with high gelsolin) was confirmed by the absence of rhodaminephalloidin staining. We suggest amphibious refraction and protection from UV irradiation and desiccation in air as selective constraints for the specializations of the *Anableps* dorsal cornea.—Swamynathan, S. K., Craw-ford, M. A., Robison, W. G., Jr., Kanungo, J., Piatigorsky, J. Adaptive differences in the structure and macromolecular compositions of the air and water corneas of the "four-eyed" fish (*Anableps anableps)*.

Keywords

amphibious vision; gelsolin; crystallin

The cornea is a multifunctional organ. Besides being a transparent protective covering at the ocular surface in terrestrial animals, it serves a refractive role as a result of its curvature (1)

[1]Correspondence: Laboratory of Molecular and Developmental Biology, National Eye Institute, National Institutes of Health, 7 Memorial Dr., Bldg. 7, Room 100A, Bethesda, MD 20892, USA. joramp@nei.nih.gov.

and the difference in the refractive indices of air (1.0) and cornea (~1.37–1.4 in humans) (2). In contrast, the function of cornea in aquatic animals is largely limited to providing transparency and protection from the environment, since the refractive indices of water (1.33) and the cornea (~1.36–1.4 in trout and hooded seal) (3, 4) are similar. When the two surfaces of cornea are parallel to each other, a small difference in refractive index between the anterior surface of cornea and water would be counterbalanced by the comparable difference between the posterior surface of cornea and aqueous humor. A similar counterbalancing effect is not observed in corneas exposed to air, since the difference in refractive index between the anterior surface of cornea and air is far greater than the difference in refractive index of posterior surface of cornea and aqueous humor. Due to the large difference in the refractive indices of air and water, eyes that must function in both have to deal with hyperopia in water and myopia in air. Such demands of amphibious vision have resulted in various adaptations in the structure of cornea as well as in the accommodative ability of the lens (4–12). The goal of the present investigation was to search for additional adaptive differences in the structure and macromolecular compositions of a cornea designed to function in air and water.

Anableps anableps, the “four-eyed” fish, is a member of the family Anablepidae, order Cyprinodontiformes, super-order Acanthopterygii. These tropical fish usually live at the surface of brackish water, with the dorsal half of their eyes exposed to air and the ventral half exposed to water (13–15). Two medial extensions of the iris overlap at the center and divide the pupil into two distinct parts: the dorsal pupil for aerial vision and the ventral pupil for aquatic vision. The shorter axis of the pyriform lens is used for aerial vision while the longer axis is used for aquatic vision. The dorsal cornea is thicker than the ventral cornea (13–15). The ultrastructure and protein composition of different tissues within the *Anableps* eye have not been characterized in detail despite the fact that they provide a unique opportunity to study structural and functional adaptations to meet the demands of amphibious vision.

We previously demonstrated abundant expression of gelsolin in the corneal epithelial cells of zebrafish (*Danio rerio*), rosey barb (*Barbus conchonius*), and tricolor shark (*Balantiocheilus melanopterus*) (16). Abundant expression of gelsolin has not been detected in the cornea of any of the terrestrial organisms studied so far. Considering the unique habitat of *Anableps*, we wanted to test whether gelsolin is abundantly expressed in its corneal epithelium, and if so, if it shows a differential pattern of expression in the dorsal and ventral corneal epithelia.

To facilitate comparative studies aimed at understanding the physiology, development, and evolution of vertebrate cornea, we provide here the first detailed description of the ultrastructure of the cornea of *Anableps* and zebrafish at the level of light microscopy and transmission electron microscopy. To understand the adaptation of *Anableps* eyes for amphibious vision at the air/water interface, we have identified differences in the structure and protein and glycogen composition between the dorsal and ventral cornea exposed to air and water, respectively. We show that the most abundant water-soluble proteins in the *Anableps* cornea are gelsolin and actin, earlier shown to be the abundant proteins in the zebrafish cornea (16). Our results demonstrate subspecialization within a single cornea to meet the demands of existence in a unique niche and suggest that gelsolin was already

recruited for abundant expression in the cornea in a common ancestor of *Anableps* and zebrafish.

MATERIALS AND METHODS

Source, culture, and anesthesia of fish

Adult *Anableps anableps* from British Guyana were obtained through Nova Tropicals (Alexandria, VA, USA). They were 7–10 cm long from anterior to posterior extremities at the time of analysis. They were kept for short periods of time at 30°C in aerated salt water with a specific gravity of 1.022 prepared by dissolving Instant Ocean (Aquarium Systems, Mentor, OH, USA) in tap water. Adult zebrafish were obtained from the lab stock maintained according to the regulations of the animal care and use committee of the NEI and were 1.0–1.25 inches in length. The fish were euthanized in water containing MS222 (a methanesulfonate salt of 3-aminobenzoic acid ethyl ester, Sigma Chemical Company, St. Louis, MO, USA) at a concentration of 50 mg/100 mL.

Light microscopy

For light microscopy, eyeballs were dissected out of the freshly euthanized fish and immediately submerged in fresh 4% paraformaldehyde (Sigma) in phosphate-buffered saline (PBS). After fixing for a minimum of 24 h at 4°C, they were embedded in glycol methacrylate (Polysciences, Warrington, PA, USA) for 2 μ-thin sections used for staining with hematoxylin and eosin, periodic acid-Schiff's (PAS) procedure, or toluidine blue (all from Sigma). Light microscopy was performed with a Zeiss Axioplan 2 microscope and the images captured using Spot RT color camera (Diagnostic Instruments, Inc., San Diego, CA, USA). The radius of curvature (r) of different segments of the cornea and the lens was calculated using the equation $r = (h^2+(w/2)^2)/2h$, where h denotes the height of the segment and w the width. The ocular measurements given in Table 1 are average values based on measurements from four different fish eyes.

Transmission electron microscopy

For transmission electron microscopy, the eyeballs were fixed in a solution containing 2.5% glutaraldehyde, 6% sucrose, 50 mM sodium cacodylate buffer (pH 7.2) for a minimum of 24 h at room temperature. Ultrathin sections were collected on 300 mesh grids and stained with uranyl acetate and lead citrate. Images were captured with a JEM-100CX electron microscope (JEOL USA, Inc., Peabody, MA, USA).

Protein electrophoresis, amino-terminal sequencing, immunoblotting, and immunohistochemistry

Water-soluble proteins from dissected corneal epithelia were extracted (16) and quantified by bicinchoninic acid method (Pierce, Rockford, IL, USA). Equal amounts of protein were separated by electrophoresis in sodium dodecyl sulfate-poly-acrylamide (SDS-PAGE) gels and transferred to PVDF membranes following the protocol suggested by the manufacturer (Invitrogen, Carlsbad, CA, USA). The gels were stained with Magic Blue (MTR Scientific, Gaithersburg, MD, USA) and scanned with the Alpha Innotech gel documentation system using ChemiImager software. Gel slices containing protein bands were rinsed twice for 1

min each, in 50% acetonitrile in water and shipped in dry ice to the Harvard Microchemistry facility (Cambridge, MA, USA) for digestion with trypsin, elution from the gel and purification of peptides by HPLC. The amino termini of the peptides were sequenced by the Edman degradation method or mass spectrometry.

Proteins separated by SDS-PAGE were transferred to a PVDF membrane and blocked with 5% nonfat dry milk in PBST (PBS with 0.1% Tween 20) for 1 h. Immunoblotting was performed using mouse anti-human gelsolin monoclonal antibodies (Research Diagnostics Inc., Flanders, NJ, USA; 1 to 1000 dilution in PBST). Horseradish peroxidase-coupled anti-mouse IgG (Amersham Biosciences, Piscataway, NJ, USA) at 1 to 2000 dilution was used as a secondary antibody. Immunoreactive bands were identified by X-ray autoradiography after incubation with Super Signal West Pico solutions (Pierce).

For immunohistochemistry, 10 μm-thick sections from paraformaldehyde fixed, paraffin embedded eyes were used. The sections were treated with xylene, hydrated using decreasing concentrations of ethanol, washed three times for 5 min each with PBS, blocked with 10% sheep serum in PBST for 1 h at room temperature, washed twice with PBST for 5 min each, incubated with the primary antibodies (mouse anti-human gelsolin monoclonal antibodies (1 to 50 dilution in blocking solution) for 1 h at room temperature, washed thrice with PBST for 10 min each, incubated with secondary antibodies (Cy-3-coupled goat anti-mouse IgG antibodies, Jackson Immunoresearch Laboratories, Inc., West Grove, PA, USA) at 1 to 100 dilution for 1 h at room temperature, washed thrice with PBST for 10 min each, mounted with anti-fade gel/mount (Biomeda Corp, Foster City, CA, USA), and observed with a Zeiss Axioplan 2 fluorescence microscope.

Rhodamine-phalloidin staining

Sections (10 μm-thick) from paraformaldehyde fixed, paraffin embedded eyes were stained with rhodamine-phalloidin following the protocol suggested by the manufacturer (Molecular Probes, Eugene, OR, USA). Paraffin was removed from the sections using xylene, then sections were hydrated using decreasing concentrations of ethyl alcohol. The slides were washed twice with PBS, treated with acetone at –20°C for 3 min, rinsed in PBS, and incubated at room temperature with 1% BSA for 30 min. Finally, the sections were stained with rhodamine-phalloidin (5 units/mL of 1% BSA) for 20 min, washed in PBS, mounted with anti-fade gel/mount, and observed using a rhodamine filter in a Zeiss Axioplan 2 fluorescence microscope. Digital photographs were taken using a Spot RT camera (Diagnostic Instruments) attachment and further processed using Adobe Photoshop software.

Glycogen estimation

The amyloglucosidase method (17) was used to estimate the amount of glycogen in the corneal epithelium. Water-soluble extract was incubated with 0.1 M NaOH at 80°C for 10 min to destroy background glucose and hexose monophosphates. The samples were neutralized with 0.1 M HCl, 0.2 M citric acid, and 0.2 M Na_2HPO_4, then incubated with amyloglucosidase (Sigma) for 1 h at room temperature. Glucose was estimated by spectrophotometry at 340 nm by the method of Passonneau and Lowry (18).

RNA isolation, cDNA cloning, and sequencing

Total RNA was isolated from the corneal epithelial cells by using the RNEasy mini kit (Qiagen, Valencia, CA, USA). Degenerate, mixed oligonucleotide primers #1334 (5′GG(A/G)TCCCA(A/T/G/C)CC(A/G)TG(A/G)AACCA 3′) and #1338 (5′GA(T/C)AA(A/G)GC(A/T/G/C)CC(A/T/G/C)GT(A/T/G/C)GA(T/C)CC 3′) designed from the aminoterminal sequence of the peptides GT-149 and GT-141, respectively, were used to amplify a 900 bp fragment from the *Anableps* gelsolin cDNA by RT-PCR using total RNA from the corneal epithelium. Sequence of this clone was used to design the primers #1663 (5′GCACCAGGTAACAGTCCCCTC-CATAGAAGTGCCC 3′) and #1664 (5′GGCAACTGACGAT-GTCATGGTTCTGGACACGTGGG 3′) needed to amplify the 5′ and 3′ ends of the cDNA by RACE, using the SMART RACE cDNA amplification kit (Clontech, Palo Alto, CA, USA). DNA was sequenced by Big Dye chemistry (Perkin Elmer, Boston, MA, USA) using the ABI Prism 310 genetic analyzer automated sequencer. The assembled *Anableps* gelsolin cDNA sequence and the deduced amino acid sequence were submitted to NCBI under accession number AY227447.

RESULTS

Anatomy of *Anableps* and zebrafish corneas

The spherical eyeball of *Anableps* is relatively large with an external diameter of 4–5 mm (Fig. 1*A*, Table 1). The pyriform lens is positioned closer to the dorsal cornea and retina than to the ventral cornea and retina. The dorsal cornea is thicker than the ventral cornea, due to the increased number of cell layers in the epithelium (Fig. 1*B, C*, Table 1). The stroma is thinner in the dorsal than the ventral cornea. The cornea is thickest at the center, where the stroma bulges posteriorly (Fig. 1*D*). Radius of curvature of the dorsal and ventral cornea estimated from the ocular measurements (Table 1) showed that the dorsal cornea is flatter than the ventral cornea. The pigmented strip that runs horizontally across the cornea, along the air/water interface is in the stroma, ~10–15 μm posterior to Bowman's membrane (Fig. 1*D*). This strip of pigmented cells along with the flaps of iris may help reduce the optical noise generated due to light scatter and total internal reflection at the water surface, resulting in the formation of two distinct images on the ventral and dorsal retinas, respectively.

In comparison, the zebrafish eyes are relatively small with a diameter of ~2 mm and possess a uniformly thin cornea, unlike the variably thick corneas of *Anableps* (Fig. 1*E*, Table 1). There are only three to four layers of cells in the zebrafish corneal epithelium, which is comparable in thickness to the underlying stroma (Fig. 1*E, F*, Table 1). The zebrafish corneal epithelial cells are smaller in size (~4 μm) than the *Anableps* corneal epithelial cells (~8–20 μm, depending on the location within the epithelium).

Bowman's membrane and glycogen content of *Anableps* and zebrafish corneas

To test whether any difference exists within Bowman's membrane and Descemet's membrane in different parts of the *Anableps* cornea, we stained the *Anableps* eye sections with PAS reagent (Fig. 2). Bowman's membrane was stained darkly in the dorsal cornea and lightly in the ventral cornea (Fig. 2*A, B*). In the pigmented region of the cornea, Bowman's membrane was lightly stained, if at all (Fig. 2*C*). Descemet's membrane was lightly stained

in all the three regions of the *Anableps* cornea examined. In the zebrafish cornea, both Bowman's and Descemet's membranes were weakly stained (Fig. 2*D*).

Unexpectedly, the dorsal corneal epithelial cells were intensely stained with PAS, indicating that they harbor abundant quantities of glycogen (Fig. 2*A*) compared with the ventral corneal epithelial cells (Fig. 2*B*). The basal epithelial cells of the dorsal cornea were stained darker than the surface epithelial cells. The epithelial cells at the air/water junction (directly anterior to the pigmented strip) were stained weaker than the epithelial cells on either the dorsal or ventral side (Fig. 2*C*). In comparison, the zebrafish corneal epithelial cells showed uniformly weak staining with PAS, indicating less glycogen (Fig. 2*D*). The amount of glycogen in the water-soluble extracts from the *Anableps* dorsal and ventral corneal epithelia and the zebrafish corneal epithelium quantified as described (17) was 0.159, 0.011, and 0.0065 μg/μg water-soluble proteins, respectively.

Ultrastructure of *Anableps* and zebrafish corneas

Results of transmission electron microscopy of different regions of the *Anableps* cornea are presented in Fig. 3. In the dorsal cornea, the superficial layers of epithelial cells possess numerous vacuoles and larger nuclei and are flatter and smaller than the cells in the underlying layers (Fig. 3*A, B*). The basal epithelial cells are columnar in the dorsal and central region, but are smaller and spherical in the ventral region of the cornea (Fig. 3*B–H*). More desmosomes are present between the epithelial cells in the central pigmented cornea than in either the dorsal or the ventral cornea. The thickness of Bowman's membrane is ~0.5 μm and 0.75 μm in the dorsal and ventral cornea, respectively. Within the pigmented cornea, Bowman's membrane is very thin and is absent in some places (Fig. 4*A–C*). Hemidesmosomes are present in abundance at the surface of the Bowman's membrane in all three regions of the cornea where the basal epithelial cells are attached. It is interesting that Bowman's membrane found in primates, fish, and chickens is not believed to be present in other species.

Lamellae of collagen fibers are ~1.0 μm thick in the dorsal stroma. They are well organized, tightly packed, branched, and arranged at right angles between layers (Fig. 4*A*). The lamellae in the ventral stroma appear thinner (~0.5 to 0.75 μm, Fig. 4*B*). Collagen fibers in between the pigmented strip and Bowman's membrane are variable in thickness and not as organized as in the rest of the stroma (Fig. 4*C*). Curiously, the lamellae in between the pigmented cells appear more organized and uniformly thick at ~1.0 to 1.5 μm (Fig. 4*D*). The intracellular pigmented granules are 0.3 to 0.5 μm in diameter. There are two kinds of granules: one electron opaque and the other, electron translucent (Fig. 4*D*).

Descemet's membrane and the associated endothelial cells appear similar in different regions of the cornea (Fig. 3*C, F, I*). Descemet's membrane is on average 1.0 μm thick in the dorsal cornea, 0.75 μm thick in the ventral cornea, and 1.25 μm thick in the pigmented cornea. The endothelial cells arranged in a single cell layer are flat, only ~1.5 to 2.0 μm thick, with very small nuclei in all the three regions of the cornea (Fig. 3*C, F, I*).

Compared with the *Anableps* cornea, the zebrafish cornea is thin, with a total thickness of ~15 to 20 μm (Fig. 5). Thickness of the epithelium and the stroma is ~8–10 μm and ~6–8

μm, respectively. The epithelium consists of three or four layers of flat and well spread out cells. The lamellae of collagen fibers, each ~200 nm thick, are arranged at right angles at a regular interval, and are not branched as in *Anableps*. There is a single layer of flattened cells (~300 nm thick) ~500 nm above Descemet's membrane. The nature and the origin of these cells are not known. The endothelium comprises a single cell layer, ~1.0 μm thick (Fig. 5). Ocular measurements made from light microscopy (Fig. 1) and electron microscopy (Figs. 3, 4, 5) of *Anableps* and zebrafish eyes are summarized in Table 1.

Water-soluble protein profiles of *Anableps* dorsal and ventral corneal epithelia

SDS-PAGE profiles of the water-soluble proteins from the dorsal and ventral corneal epithelia were similar except for the relative amount of an abundant 80 kDa protein, which accounted for 38% and 21% of the water-soluble proteins in the dorsal and ventral corneal epithelium, respectively (Fig. 6*A*). Amino acid sequence of the amino termini of tryptic peptides from this protein showed homology to gelsolin from different species (Fig. 6*B*). An immunoblot of water-soluble proteins from the cornea and other tissues of *Anableps* confirmed cross-reactivity with gelsolin and demonstrated its presence in lower amounts in the digestive tract, gill and brain (Fig. 6*C, D*). The second most abundant protein in the corneal extracts migrated at 40 kDa and was present in roughly equal amounts (~15%) in the dorsal and ventral epithelial cells (Fig. 6*A*). This protein was identified by mass spectrometry as actin (data not shown).

Immunohistochemistry with a monoclonal anti-human gelsolin antibody confirmed the abundant expression of gelsolin in the *Anableps* corneal epithelium (Fig. 7). Images obtained at higher magnification showed that gelsolin is concentrated in the cytoplasm (Fig. 7*D*). The concentration of gelsolin was uniform across the different layers of the dorsal epithelium. In addition to the corneal epithelia, gelsolin staining was found in the lens capsule and the iris (Fig. 7*B*). However, since the Western blot using the same antibody did not detect gelsolin in the lens proteins (Fig. 6*D*), detection of gelsolin in the lens capsule by immunohistochemistry could be an artifact of the procedure.

Anableps and zebrafish gelsolin

Gelsolin cDNA was cloned by RT-PCR using total RNA from the *Anableps* dorsal corneal epithelium. The *Anableps* gelsolin cDNA sequence is 75% identical to that of zebrafish (16). The 3′ untranslated region is only 26 bp in the *Anableps* gelsolin cDNA compared with 273 bp in the zebrafish gelsolin cDNA. Although we could not identify a well-conserved polyadenylation signal sequence, a poly (A) tail is present at the 3′ end of the *Anableps* gelsolin cDNA. An open reading frame encoding a protein of 712 amino acids was identified within this cDNA. The deduced amino acid sequence of *Anableps* gelsolin is 57% identical to the zebrafish gelsolin.

Members of the gelsolin family of proteins possess multiple repeats of a 93 amino acid domain (the gelsolin homology domain) that are involved in Ca^{2+} and actin binding (Reference ID Smart00262 in NCBI conserved domain database). Six such repeats with variable degrees of sequence similarity are present in the *Anableps* gelsolin (Fig. 8). The highest degree of divergence occurs in the amino-terminal domain, which is 25% identical to

the conserved gelsolin homology domain sequence. *Anableps* and zebrafish gelsolin lack the amino-terminal head piece of 50 amino acids found in human and pig gelsolin (Fig. 8).

Actin severing ability of *Anableps* gelsolin

Gelsolin binds and severs filamentous F-actin to monomeric G-actin (19, 20). The actin severing ability of *Anableps* gelsolin was tested indirectly by staining the *Anableps* eye sections with rhodamine-phalloidin, a selective stain for F-actin. Sections of the mouse cornea, which contain relatively little gelsolin, were included as positive control for F-actin (16). As expected, the sections of mouse cornea were darkly stained with rhodamine-phalloidin, indicating the presence of F-actin (Fig. 9*A*). In contrast, the *Anableps* corneal epithelia were not stained under identical conditions, suggesting little or no F-actin (Fig. 9*D, F*) despite the abundance of actin in these cells, as shown by SDS-PAGE (Fig. 6). These data are comparable to those obtained earlier for the zebrafish cornea (16) and are consistent with *Anableps* gelsolin having actin severing ability.

DISCUSSION

The present study characterizes novel features of the amphibious *Anableps* eye. These include the radius of curvature, thickness, ultrastructure, protein composition, and glycogen content of different layers of the dorsal and ventral cornea exposed to air and water, respectively. Furthermore, we identified gelsolin and G-actin as the two most abundantly expressed water-soluble proteins in the *Anableps* cornea, and cloned and characterized the cDNA encoding gelsolin.

Our previous studies showed that the actin severing protein gelsolin comprises ~50% of the water-soluble protein of the zebrafish cornea and is concentrated in the four- to five cell-layered corneal epithelium (16). The corneal function of the abundant gelsolin in *Anableps* or zebrafish remains to be determined. Recent work from our laboratory has demonstrated that gelsolin acts as a dorsalizing factor during the early developmental stages of zebrafish embryos, before it accumulates in the cornea (21). The abundance of gelsolin in the *Anableps* corneal epithelium represents another example of the taxon specificity of the abundant intracellular corneal proteins (22, 23). We were surprised to find in *Anableps* that the proportion of gelsolin was higher in the dorsal cornea exposed to air (38%) than in the ventral cornea exposed to water (21%), since gelsolin is so prevalent in the zebrafish aquatic cornea and present in very low amounts in the cornea of terrestrial species. It thus appears that the accumulation of gelsolin in the cornea is not disadvantageous when the tissue is exposed to air. The fact that gelsolin is the major water-soluble corneal protein of *Anableps* indicates that the recruitment of gelsolin as a major corneal protein in fish occurred at least 100 million years ago, the time of divergence between zebrafish and *Anableps* (24, 25). It would be of interest to determine whether gelsolin is also a dominant protein in the ancient sea lamprey primary spectacle (dermal cornea), which appears generally similar to the cornea of fish and higher vertebrates (26, 27).

The most striking difference we observed between the dorsal and ventral cornea of *Anableps* was the thickness of the epithelium. There were >20 layers of epithelial cells in the dorsal cornea, while the relatively thin ventral cornea contained ~5 epithelial cell layers.

Considering the angle at which the dorsal cornea is positioned, facing upward and directly exposed to the sunlight, more layers of epithelial cells may provide additional chromophores (in the form of water, nucleic acids and proteins) to absorb UV light. High concentrations of glycogen, as present in the dorsal corneal epithelium of *Anableps*, have previously been observed in the rabbit cornea (28) and pigeon lens (29). The rabbit corneal epithelial cell glucose and glycogen concentrations increased upon exposure to UV radiation (30). Perhaps *Anableps* dorsal corneal epithelial cells also accumulate glycogen in response to UV radiation. It is also possible that the increased thickness of the dorsal corneal epithelium has a refractive role aiding vision in air, as might the abundance of gelsolin and glycogen in the thickened dorsal corneal epithelium. Another possibility is that the highly stratified dorsal corneal epithelium of *Anableps* protects against desiccation when exposed to air, since there are no tear film or eyelids used to keep the corneal surface moist as in terrestrial vertebrates. It is noteworthy that the corneal epithelial cells in mice stratify when exposed to light and air upon eye opening, and in vitro airlift cultures of corneas undergo more epithelial cell stratification than submerged cultures (31). The accumulation of glycogen, as in the dorsal corneal of *Anableps*, has been well correlated with desiccation resistance in *Drosophila* (32, 33).

The flatter radius of curvature of the dorsal than the ventral cornea of *Anableps* is another significant finding of the present study. The submerged ventral cornea has virtually no refractive role. By contrast, the dorsal cornea will have a refractive function in air (7, 5, 34, 10). Amphibians encounter myopia in air and hyperopia in water due to the loss of refractive ability in water (8). Thus, the relatively flattened dorsal cornea of *Anableps* appears to be a morphological adaptation to reduce refraction at the air/cornea interface. Similarly, flattened corneas are present in the intertidal fish *Mnierpes macrocephalus* (8) and the Atlantic flying fish *Cypselurus heterurus* (7). Adaptations to an air/water visual existence include increased accommodation in the sea otter (5) and the diving sea cormorant (34). Penguins have incorporated both of these features: they possess a flattened cornea and an ability to accommodate well to minimize the optical effects of an amphibious existence (10).

In addition to the flattened cornea, the shape and placement of the lens are thought to allow *Anableps* to focus properly in air and water (11, 12, 14, 15). The light from the air passes through the shorter axis of the pyriform lens with a relatively flat surface while the light from the water passes through the longer axis of the lens with a higher surface curvature. In the aquatic axis of vision, the lens bears the burden of refraction; yet it is positioned very close to the dorsal retina, making it difficult to conceive how *Anableps* can focus properly on underwater objects while cruising at the water surface. Furthermore, *Anableps* demonstrates an optomotor response only in the aerial axis of vision (35). Therefore, it is possible that the *Anableps*, while having acute vision in air from the dorsal cornea, cannot focus well underwater from the ventral cornea and only detects differ ences in the intensity of underwater light. Indeed, when submerged, *Anableps* may depend on the dorsal cornea itself for acute vision.

Finally, accommodation in amphibious vision occurs both by movement and shape change of the lens. It has been suggested that *Anableps* can accommodate in the aquatic axis of vision (14), but nothing is known about its ability to accommodate in the aerial axis of

vision. We note here that a large cavernous choroidal tissue is present beneath the ventral retina that receives light from the air (Fig. 1). Similar tissue was not found beneath the dorsal retina. Involvement of choroids in accommodation is known: the chick eye is capable of modulating its refractive state by pushing or pulling the retina by changing the thickness of the choroids (36). By analogy, we propose that *Anableps* may focus in the air by moving the ventral retina closer to or away from the lens by filling or withdrawing blood from the choroid chamber. Yet another possibility, which stems from the fact that choroid is involved in regulating oxygen supply to the retina (37), is that the extent of retinal vasculature and, consequently, requirement for additional oxygen supply may differ between the dorsal and ventral retinas. The choroid may in such a scenario supply adequate amounts of oxygen to the ventral retina. Further experiments are needed to test these possibilities.

In conclusion, the divided corneas, one for aquatic vision and one for aerial vision, of *Anableps* provide a remarkable example of subspecialization of the eye for adaptation to a unique niche at the interface of air and water.

Acknowledgments

We would like to thank Ms. Carol Boelke of Nova Tropicals, Alexandria, VA, for procuring *Anableps* from British Guyana for us and Dr. William S. Lane and other members of the Harvard Microchemistry facility, Cambridge, MA, for their help in identifying the corneal proteins. We thank Ms. Barbara Norman for help throughout the course of this study, Drs. Zbynek Kozmik, Janine Davis, David Nees, Zhengping Xu, and Richard B. Hough for their critical comments on the manuscript, and Dr. P. Santhoshkumar for drawing our attention to the link between desiccation resistance and glycogen accumulation.

References

1. Patel S. Refractive index of the mammalian cornea and its influence during pachometry. Ophthalmic Physiol Opt. 1987; 7:503–506. [PubMed: 3454930]
2. Patel S, Marshall J, Fitzke FW III. Refractive index of the human corneal epithelium and stroma. J Refract Surg. 1995; 11:100–105. [PubMed: 7634138]
3. Leonard DW, Meek KM. Refractive indices of the collagen fibrils and extrafibrillar material of the corneal stroma. Biophys J. 1997; 72:1382–1387. [PubMed: 9138583]
4. Sivak JG, Howland HC, West J, Weerheim J. The eye of the hooded seal, *Cystophora cristata*, in air and water. J Comp Physiol [A]. 1989; 165:771–777.
5. Murphy CJ, Bellhorn RW, Williams T, Burns MS, Schaeffel F, Howland HC. Refractive state, ocular anatomy, and accommodative range of the sea otter (Enhydra lutris). Vision Res. 1990; 30:23–32. [PubMed: 2321364]
6. Jermann T, Senn DG. Amphibious vision in *Coryphoblennius galerita* L. (Perciformes). Experientia. 1992; 48:217–218. [PubMed: 1547846]
7. Knowles F, Vollrath L, Nishioka RS. Air and water vision of the atlantic flying fish, Cypselurus heterurus. Nature (London). 1967; 214:307–309. [PubMed: 6034254]
8. Graham JB, Rosenblatt RH. Aerial vision: unique adaptation in an intertidal fish. Science. 1970; 168:586–588. [PubMed: 5436592]
9. Sivak J, Howland HC, McGill-Harelstad P. Vision of the Humboldt penguin (*Spheniscus humboldti*) in air and water. Proc R Soc Lond B Biol Sci. 1987; 229:467–472. [PubMed: 2881308]
10. Howland HC, Sivak JG. Penguin vision in air and water. Vision Res. 1984; 24:1905–1909. [PubMed: 6534014]
11. Walls, GL. The Vertebrate Eye and its Adaptive Radiation. The Cranbrook Institute of Science; Bloomfield Hills, MI: 1942.
12. Land, MF., Nilsson, DE. Animal Eyes. Oxford University Press; New York: 2002.

13. Schwassmann HO, Kruger L. Experimental analysis of the visual system of the four-eyed fish *Anableps microlepis*. Vision Res. 1966; 5:269–281. [PubMed: 5905869]
14. Sivak JG. Optics of the eye of the “four-eyed fish” (Anableps anableps). Vision Res. 1976; 16:531–534. [PubMed: 941438]
15. Schwab IR, Ho V, Roth A, Blankenship TN, Fitzgerald PG. Evolutionary attempts at 4 eyes in vertebrates. Trans Am Ophthalmol Soc. 2001; 99:145–156. [PubMed: 11797302]
16. Xu YS, Kantorow M, Davis J, Piatigorsky J. Evidence for gelsolin as a corneal crystallin in zebrafish. J Biol Chem. 2000; 275:24645–24652. [PubMed: 10818094]
17. Adamo KB, Graham TE. Comparison of traditional measurements with macroglycogen and proglycogen analysis of muscle glycogen. J Appl Physiol. 2002; 84:908–913.
18. Passonneau, J., Lowry, O. Enzymatic Analysis: A Practical Guide. Humana; Clifton, NJ: 1993. p. 177-178.
19. Kwiatkowski DJ. Functions of gelsolin: motility, signaling, apoptosis, cancer. Curr Opin Cell Biol. 1999; 11:103–108. [PubMed: 10047530]
20. Sun HQ, Yamamoto M, Mejillano M, Yin HL. Gelsolin, a multifunctional actin regulatory protein. J Biol Chem. 1999; 274:33179–33182. [PubMed: 10559185]
21. Kanungo J, Kozmik Z, Swamynathan SK, Piatigorsky J. Gelsolin is a dorsalizing factor in zebrafish. Proc Natl Acad Sci USA. 2003; 100:3287–3292. [PubMed: 12629212]
22. Piatigorsky J. Gene sharing in lens and cornea: facts and implications. Prog Retin Eye Res. 1998; 17:145–174. [PubMed: 9695791]
23. Piatigorsky J. Engima of the abundant water-soluble cytoplasmic proteins of the cornea. Cornea. 2001; 20:853–858. [PubMed: 11685065]
24. Nelson, JS. Fishes of the World. Wiley; New York: 1994.
25. Muller F, Blader P, Strahle U. Search for enhancers: teleost models in comparative genomic and transgenic analysis of *cis* regulatory elements. Bioessays. 2002; 24:564–572. [PubMed: 12111739]
26. Van Horn DL, Edelhauser HF, Schultz RO. Ultrastructure of the primary spectacle and cornea of the sea lamprey. J Ultrastruct Res. 1969; 26:454–464. [PubMed: 5776315]
27. Pederson HJ, Van Horn DL, Edelhauser HF. Ultrastructural changes associated with loss of transparency in the primary spectacle and cornea of spawning sea lamprey. Exp Eye Res. 1971; 12:147–150. [PubMed: 5120345]
28. Amemiya T, Yoshida H. Electron histochemical study on synthesis and breakdown of glycogen in the rabbit cornea. Acta Histochem. 1978; 62:302–309. [PubMed: 104532]
29. Lo WK, Kuck JF, Shaw AP, Yu NT. The altricial pigeon is born blind with a transient glycogen cataract. Exp Eye Res. 1993; 56:121–126. [PubMed: 8432331]
30. Lattimore MR Jr. Effect of ultraviolet radiation on the energy metabolism of the corneal epithelium of the rabbit. Photochem Photobiol. 1989; 49:175–180. [PubMed: 2710826]
31. Zieske JD, Mason VS, Wasson ME, Meunier SF, Nolte CJ, Fukai N, Olsen BR, Parenteau NL. Basement membrane assembly and differentiation of cultured corneal cells: importance of culture environment and endothelial cell interaction. Exp Cell Res. 1994; 214:621–633. [PubMed: 7523155]
32. Folk DG, Han C, Bradley TJ. Water acquisition and partitioning *Drosophila melanogaster*: effects of selection for desiccation-resistance. J Exp Biol. 2001; 204:3323–3331. [PubMed: 11606606]
33. Gibbs AG, Chippindale AK, Rose MR. Physiological mechanisms of evolved desiccation resistance in *Drosophila melanogaster*. J Exp Biol. 1997; 200:1821–1832. [PubMed: 9225453]
34. Levy B, Sivak J. Mechanisms of accommodation in the bird eye. J Comp Physiol [A]. 1980; 137:267–272.
35. Saidel WM, Fabiane RS. Optomotor response of *Anableps anableps* depends on the field of view. Vision Res. 1998; 38:2001–2006. [PubMed: 9797946]
36. Wallman J, Wildsoet C, Xu A, Gottlieb MD, Nickla DL, Marran L, Krebs W, Christensen AM. Moving the retina: choroidal modulation of refractive state. Vision Res. 1995; 35:37–50. [PubMed: 7839608]

37. Yu DY, Cringle SJ. Oxygen distribution and consumption within the retina in vascularized and avascular retinas and in animal models of retinal disease. Prog Retin Eye Res. 2001; 20:175–208. [PubMed: 11173251]

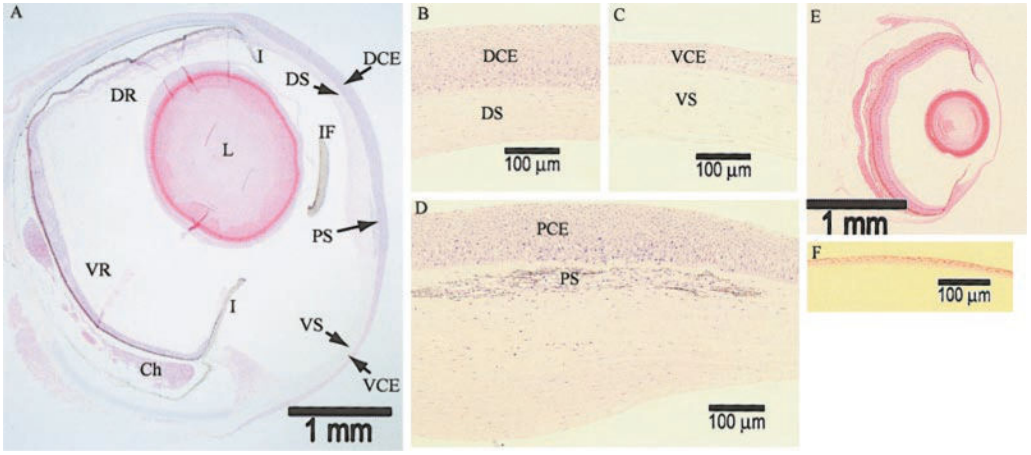

Figure 1.

Light microscopy of *Anableps* and zebrafish eyes. *A)* Bright-field microscopy of 2 µm-thick methacrylate-embedded sections stained with hematoxylin and eosin at 25× magnification. DCE, dorsal corneal epithelium; VCE, ventral corneal epithelium; PCE, pigmented corneal epithelium; PS, pigmented strip; I, iris; IF, iris flap; DS, dorsal corneal stroma; VS, ventral corneal stroma; DR, dorsal retina; VR, ventral retina; Ch, choroidal tissue; L, lens. *B)* Dorsal cornea, at 200× magnification. *C)* Ventral cornea, at 200× magnification. *D)* Central cornea bisected by the water surface, at 200× magnification. *E)* Zebrafish eye, at 25× magnification. *F)* Zebrafish cornea, at 200× magnification. Scale bars are provided for reference.

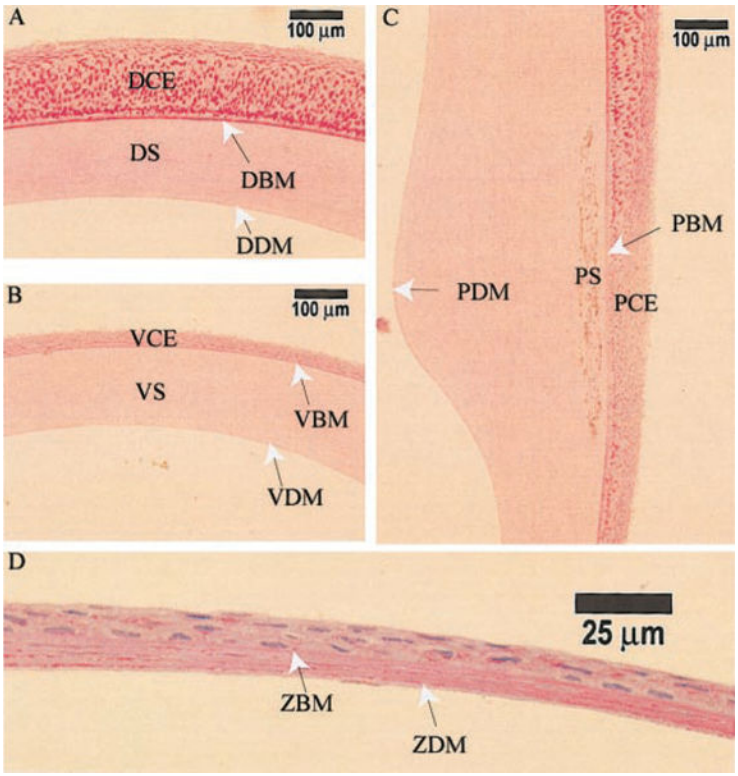

Figure 2.

Periodic acid-Schiff's reagent (PAS) staining of *Anableps* cornea. 10 μm-thick sections from paraffin embedded *Anableps* and zebrafish eyes were stained with PAS. *A)* Dorsal cornea, *B)* ventral cornea, *C)* pigmented cornea, and *D)* zebrafish cornea. DBM, dorsal Bowman's membrane; VBM, ventral Bowman's membrane; DDM, dorsal Descemet's membrane; VDM, ventral Descemet's membrane; PBM, Bowman's membrane in the pigmented cornea; PDM, Descemet's membrane in the pigmented cornea; ZBM, zebrafish Bowman's membrane; ZDM, zebrafish Descemet's membrane; the rest of the notations are as in Fig. 1.

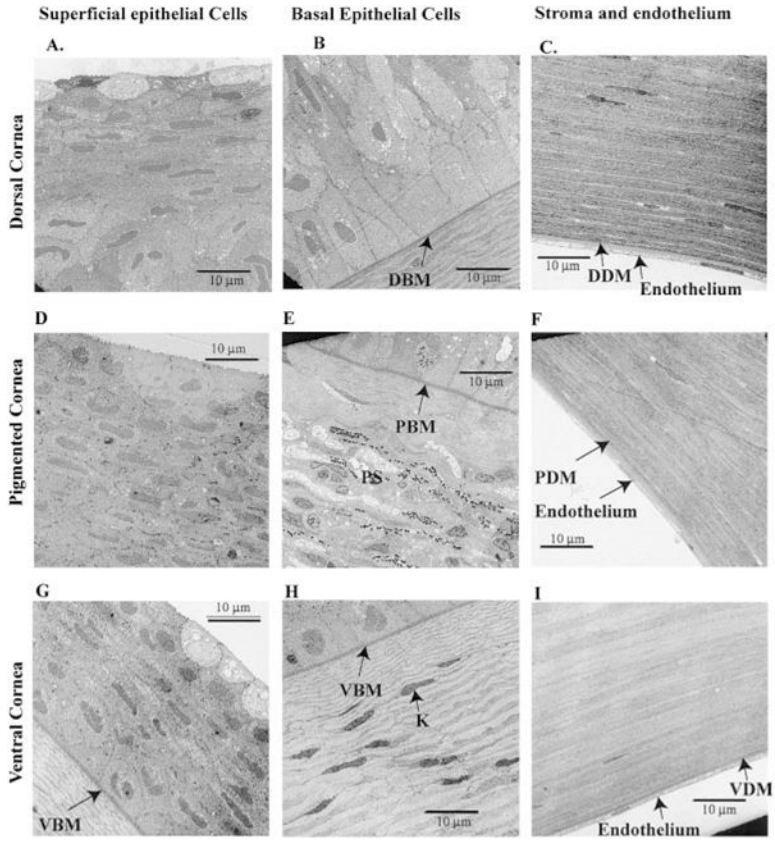

Figure 3.

Transmission electron microscopy of the *Anableps* cornea. *A)* Superficial epithelial cells from the dorsal cornea; *B)* basal epithelial cells and Bowman's membrane from the dorsal cornea; *C)* stroma, Descemet's membrane, and endothelial cells from the dorsal cornea; *D)* superficial epithelial cells from the pigmented cornea; *E)* basal epithelial cells and Bowman's membrane from the pigmented cornea; *F)* stroma, Descemet's membrane, and endothelial cells from the pigmented cornea; *G)* epithelium and Bowman's membrane from the ventral cornea; *H)* basal epithelium and Bowman's membrane from the ventral cornea; *I)* stroma, Descemet's membrane, and endothelial cells from the dorsal cornea. 3000× magnification. Notations are as in Figs. 1 and 2. Scale bars are shown.

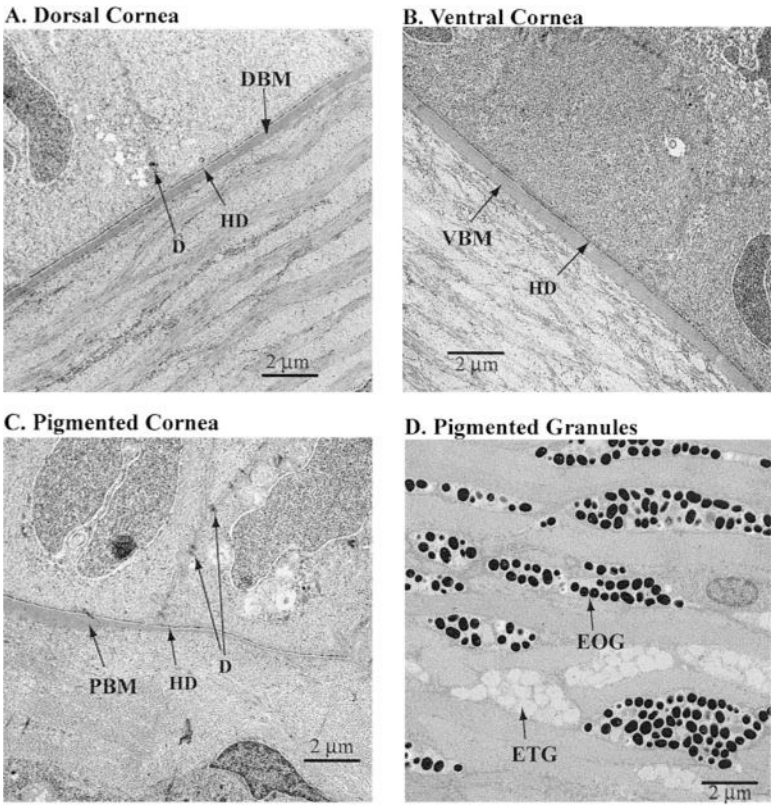

Figure 4.

Transmission electron microscopy of the *Anableps* corneal epithelial cells. *A)* Dorsal cornea. DBM, dorsal Bowman's membrane. *B)* Ventral cornea. VBM, ventral Bowman's membrane. *C)* Pigmented cornea. PBM, Bowman' membrane in the pigmented cornea is abnormally thin and almost disappears at the right-hand side. *D)* Chromocytes within the pigmented strip in the stroma, showing both the electron opaque granules (EOG) and electron translucent granules (ETG). HD, hemidesmosomes; D, desmosomes. 10,000× magnification.

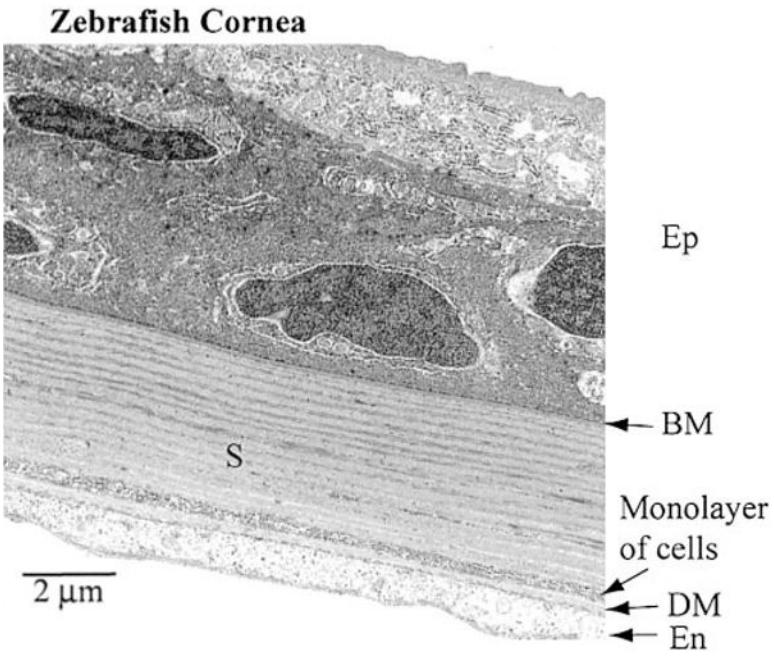

Figure 5.

Transmission electron microscopy of the zebrafish cornea. Different layers of the zebrafish cornea are shown along with the scale bar. The epithelium contains only 3–4 cell layers. Note a monolayer of cells within the stroma, ~500 nm above the Descemet's membrane. 10,000× magnification.

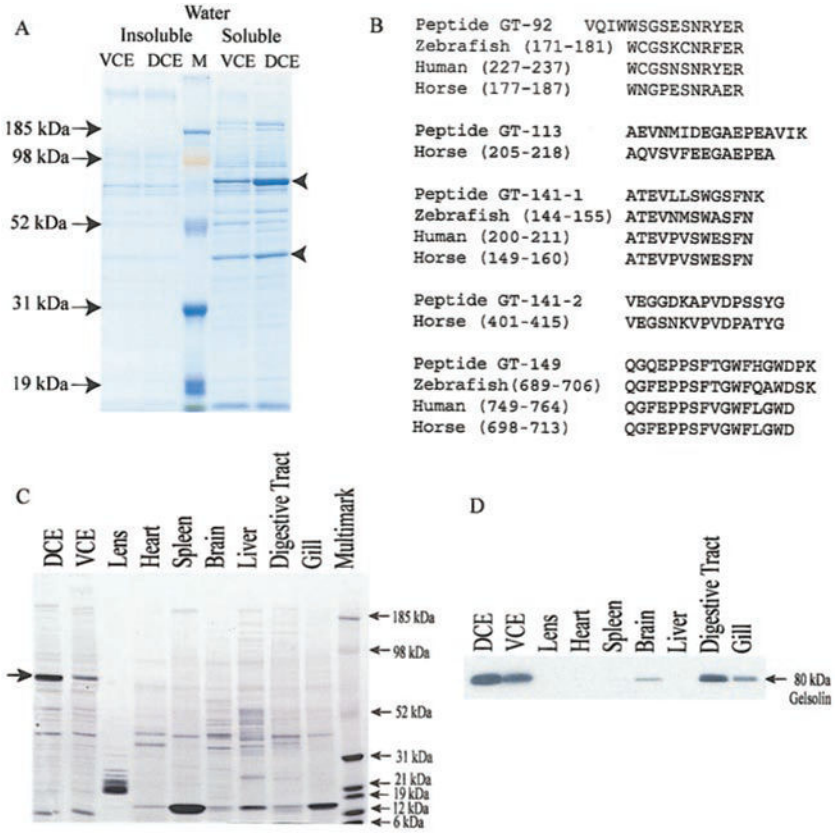

Figure 6.

Gelsolin is an abundant water-soluble protein in *Anableps* corneal epithelia. *A)* SDS-PAGE profile of water-insoluble and water-soluble proteins from *Anableps* ventral (VCE) or dorsal (DCE) corneal epithelia. M, molecular weight marker. *B)* Amino-terminal sequence of peptides GT-92, GT-113, GT-141, and GT-149 generated by trypsin digestion of the abundant 80 kDa protein, showing similarities with corresponding peptides of gelsolin protein from different species. *C)* SDS-PAGE gel of water-soluble proteins from different tissues of *Anableps* (duplicate of the gel used for Western blot in panel *D*) stained with Coomassie blue. *D)* Immunoblot showing the expression of gelsolin in different tissues of the adult *Anableps*.

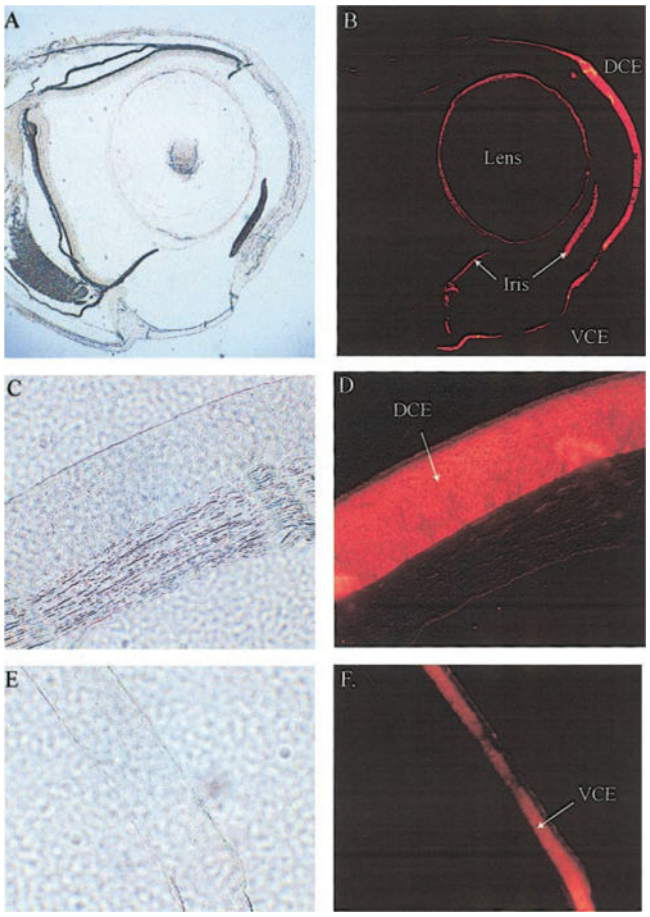

Figure 7.

Immunohistochemistry of *Anableps* eye sections. Paraformaldehyde-fixed, paraffin embedded eyes were sectioned and stained with an anti-human gelsolin antibody as described in Materials and Methods. *A, B*) Whole eye; *C, D*) dorsal cornea from *Anableps*; *E, F)* ventral cornea from *Anableps*. *A, C, E)* Bright-field photographs. *B, D, F)* Fluorescence photographs.

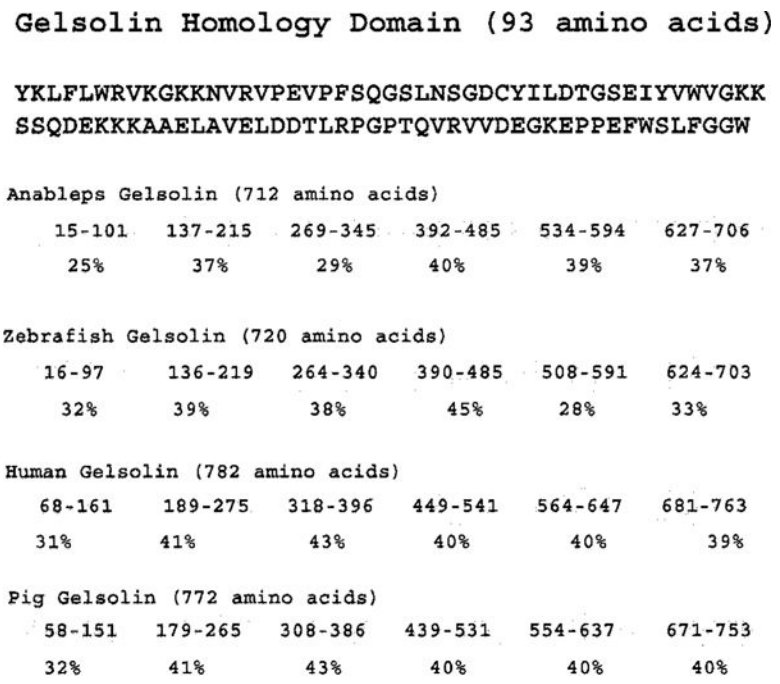

Figure 8.

Comparison of *Anableps*, zebrafish, human, and pig gelsolin homology domains. The amino acid sequence of the conserved gelsolin homology domain taken from the NCBI domain database (Reference ID smart00262) is presented at the top. Shown below are the domain structures of *Anableps*, zebrafish, human and pig gelsolin proteins in which each oval represents a domain and the numbers within each oval represent the position of amino acids within the corresponding protein contributing to that domain. The extent of sequence identity of each domain compared with the conserved gelsolin homology domain is shown below each domain in percentages. NCBI GenBank accession numbers for *Anableps*, zebrafish, human and pig geslolin are AY227447, AAF99088, P06396, and P20305, respectively.

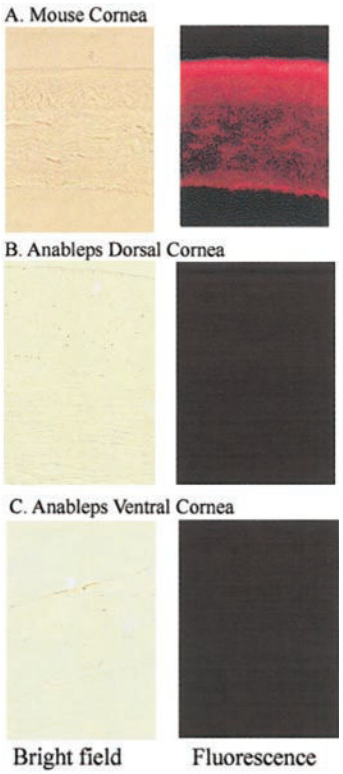

Figure 9.

Rhodamine-phalloidin staining of 10 μm sections from *Anableps* eyes. Paraformaldehyde-fixed, paraffin embedded eyes were sectioned and stained with rhodamine-phalloidin as described in Materials and Methods. *A)* Positive control mouse eye sections; *B)* dorsal cornea from *Anableps*; *C)* ventral cornea from *Anableps*. Bright-field photographs are on the left and fluorescence photographs are on the right. Note that under uniform conditions of staining and exposure, mouse cornea is strongly stained with rhodamine-phalloidin while the *Anableps* cornea is not, indicating an absence of actin microfilaments in the *Anableps* corneal epithelia.

TABLE 1

Ocular measurements in the Anableps and the zebrafish eyes[a]

Characteristic	Aerial axis, μm	Aquatic axis, μm	Zebrafish, μm
Radius of curvature[b]			
External surface of cornea	1940 (±34.6)	1630 (±87)	1237 (±195)
Lens	1206 (±45.3)	870 (±26)	420 (±37.5)
Thickness			
Corneal epithelium	148 (±3.1)	33 (±1.2)	8.75 (±1.1)
Corneal stroma	134 (±4.55)	153 (±1.2)	8.00 (±1.35)
Lens	1720 (±116)	2270 (±131)	660 (±78)
Distance			
Endothelium to lens	476 (±30)	1300 (±37.5)	73 (±6)
Lens to retina	1060 (±23)	121 (±11)	388 (±16.5)

[a]Average values of measurements from four different eyes are provided, with the standard deviation in parentheses.

[b]Radius of curvature (r) was calculated using the formula $r = (h^2+(w/2)^2)/2h$, where h is the height and w the width of the segment of cornea or lens.